
Progressive Neural Representation for Sequential Video Compilation

Haeyong Kang[†], DaHyun Kim[†], Jaehong Yoon, Sung Ju Hwang, and Chang D Yoo^{*}

Korea Advanced Institute of Science and Technology (KAIST)

{haeyong.kang, dahyun.kim, jaehong.yoon, sjhwang82, cdyoo}@kaist.ac.kr

Abstract

Neural Implicit Representations (NIR) have gained significant attention recently due to their ability to represent complex and high-dimensional data. Unlike explicit representations, which require storing and manipulating individual data points, implicit representations capture information through a learned mapping function without explicitly representing the data points themselves. They often prune or quantize neural networks after training to accelerate encoding/decoding speed, yet we find that conventional methods fail to transfer learned representations to new videos. This work studies the continuous expansion of implicit video representations as videos arrive sequentially over time, where the model can only access the videos from the current session. We propose a novel neural video representation, *Progressive Neural Representation (PNR)*, that finds an adaptive substructure from the supernet for a given video based on Lottery Ticket Hypothesis. At each training session, our PNR transfers the learned knowledge of the previously obtained subnetworks to learn the representation of the current video while keeping the past subnetwork weights intact. Therefore it can almost perfectly preserve the decoding ability (i.e., catastrophic forgetting) of the NIR on previous videos. We demonstrate the effectiveness of our proposed PNR on the neural sequential video representation compilation on the novel UVG8/17 video sequence benchmarks. The public code is available at <https://github.com/haeyong/PNR>.

1 Introduction

Neural Implicit Representation (NIR) [8, 21, 7, 26] is a research direction that aims to represent complex data, such as videos or 3D objects, as continuous functions learned by neural networks. Instead of explicitly describing data points, NIR models learn to compress high-dimensional data into a low-dimensional latent space and re-map it to a high-dimensional latent space, allowing efficient data storage, compression, and synthesis. However, individual high-dimensional data must occupy a neural network as an encoding, increasing linear memory capacity when users compress multiple target data. Neural Video Representation [8, 6] variants deal with this issue by merging different videos into a single video before training. However, they have limited transferability by design as learned models are compressed via weight pruning and quantization, and thus cannot improve the representations when new videos arrive at the model over successive time sessions. In this paper, as inspired by incremental knowledge transfer and expansion in continual learning, we investigate a practical implicit representation learning scenario with video data, dubbed *video continual learning (VCL)*, which aims to accumulate neural implicit representations for multiple videos into a single model under the condition that videos are incoming in a sequential manner.

^{*}Corresponding author, [†] Equal contribution.

Continual Learning (CL) [40, 33, 48, 13] is a learning paradigm where a model learns over a series of sessions sequentially. It aims to mimic human cognition, characterized by the ability to learn new concepts incrementally throughout a lifetime without the degeneration of previously acquired functionality. Yet, incremental training of NIR is a challenging problem since the model detrimentally loses the learned implicit representations of past session videos while encoding newly arrived ones, a phenomenon known as *catastrophic forgetting* [25]. This issue particularly matters as neural representation methods for videos encode and reconstruct the target data stream conditioned to its frame indices. Then, the model more easily ruins its generation ability while learning to continuously encode new videos due to the distributional disparities in *holistic videos* and their *individual frames*. Furthermore, the *compression phase* of neural representation makes it wayward to transfer the model to future tasks. Various approaches have been proposed to address catastrophic forgetting during continual learning, which are often conventionally classified as follows: (1) *Regularization-based methods* [19, 2, 16, 41, 28] aim to keep the learned information of past sessions during continual training aided by sophisticatedly designed regularization terms, (2) *Architecture-based methods* [47, 24, 36, 44, 17, 18] propose to minimize the inter-task interference via newly designed architectural components, and (3) *Rehearsal-based methods* [31, 4, 34, 46] utilize a set of real or synthesized data from the previous sessions and replay them. Note that rehearsal-based methods are often undesirable for continual learning on complex data since they need non-negligible memory to store high-dimensional samples in a buffer and revisit them to learn, suffering from embarrassingly large memory consumption and computational cost.

To enhance neural representation incrementally on sequential videos, we propose a novel video continual learning method coined **Progressive Neural Representation (PNR)**. Given a backbone architecture, our proposed method aims to learn adaptive subnetwork structure along with its weights to encode incoming videos at each training session. We leverage the idea from *Lottery Ticket Hypothesis (LTH)*, demonstrating sparse subnetworks preserving a dense network’s performance. However, searching for optimal subnetworks, often called *winning tickets*, during continual learning is inefficient since they require iterative training steps with repetitive pruning and retraining in each arriving task. To this end, our proposed PNR introduces a parametric score function that learns to generate binary masks to find adaptive substructures for video encoding in each training session by directly choosing top- c percent in weight ranking scores. We emphasize that PNR can find the optimal subnetwork in an online manner through joint training of the weights and structure and bypass arduous procedures in LTH, such as iterative retraining, pruning, and rewinding. Our PNR allows overlapping subnetworks with previous sessions during training to transfer the learned representation of previous videos when relevant but keeps the weights for previous video sessions frozen. Consequently, we enable the model to expand its representation space throughout consecutive video sessions continuously, ensuring maintaining the encoding and generation quality of the previous video intact (i.e., forgetting-free) even without resorting to a replay buffer to store multiple high-dimensional frames.

Our contributions can be summarized as follows:

- We suggest a practical learning scenario for neural implicit representation where the model encodes multiple videos continually in successive training sessions. Earlier NIR methods suffer from poor transferability to new videos due to the distributional shift of holistic video and frames.
- We propose a novel progressive neural representation method for a sequential video compilation. The proposed method continuously learns a compact subnetwork for each video session given a supernet backbone while preserving the generative quality of previous videos perfectly.
- We demonstrate the effectiveness of our method on multiple sequential video sessions by achieving superior performance in average PSNR and MS-SSIM without any quantitative/qualitative degeneration in reconstructing previously encoded videos during sequential video compilation.

2 Related Works

Neural Implicit Representation (NIR). Neural Implicit Representations (NIR) [26] are neural network architectures for parameterizing continuous, differentiable signals. Based on coordinate information, they provide a way to represent complex, high-dimensional data with a small set of learnable parameters that can be used for various tasks such as image reconstruction [38, 39], shape regression [10, 29], and 3D view synthesis [27, 35]. Instead of using coordinate-based

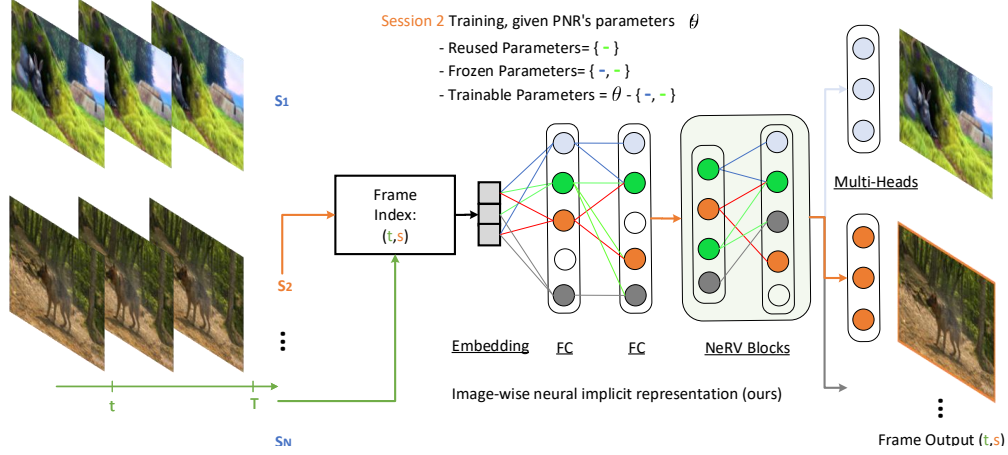


Figure 1: **Progressive Neural Representation (PNR) for Sequential Video Compilation:** Image-wise neural implicit representation taking frame and video (session) indices as input and using a sparse MLP + NeRV Blocks to output the whole image through multi-heads. We denote frozen, reused, and trainable parameters in training at session 2. Note that each video representation is colored.

methods, NeRV [8] proposes an image-wise implicit representation that takes frame indices as inputs, enabling fast and accurate video compression. NeRV has inspired further improvements in video regression by CNeRV [6], DNeRV [14], E-NeRV [21], and NIRVANA [23], and HNeRV [7]. A few recent works have explored video continual learning (VCL) scenarios for the NIR. To tackle non-physical environments, Continual Predictive Learning (CPL) [5] learns a mixture world model via predictive experience replay and performs test-time adaptation using non-parametric task inference. PIVOT [42] leverages the past knowledge present in pre-trained models from the image domain to reduce the number of trainable parameters and mitigate forgetting. CPL needs memory to replay, while PIVOT needs pre-training and fine-tuning steps. In contrast, we introduce a novel neural video representation referred to as "*Progressive Neural Representation (PNR)*", which utilizes the Lottery Ticket Hypothesis (LTH) to identify an adaptive substructure within the dense networks that are tailored to the specific video input index. Our PNR doesn't use memory, a pre-trained model, or fine-tuning for a sequential video representation compilation.

Continual Learning. Most continual learning approaches introduce extra memory like additional model capacity [20, 45] or a replay buffer [32, 3]. But, several works have focused on building memory-efficient continual learners using pruning-based constraints to exploit initial model capability more compactly. CLNP [12] selects important neurons for a given task using ℓ_1 regularization to induce sparsity and freezes them to maintain performance. And pruned neurons are reinitialized for future task training. Piggyback [24] trains task-specific binary masks on the weights given a pre-trained model. However, it does not allow for knowledge transfer among tasks, so the performance highly depends on the quality of the backbone model. HAT [36] proposes task-specific learnable attention vectors to identify significant weights per task. The masks are formulated to layerwise cumulative attention vectors during continual learning. LL-Tickets [9] recently suggests sparse subnetworks called lifelong tickets that perform well on all tasks during continual learning. The method searches for more prominent tickets from current ones if the obtained tickets cannot sufficiently learn the new task while maintaining performance on past tasks. However, LL-Tickets require external data to maximize knowledge distillation with learned models for prior tasks, and the ticket expansion process involves retraining and pruning steps. WSN [17] jointly learns the model weights and task-adaptive binary masks during continual learning. It prevents catastrophic forgetting of previous tasks by keeping the model weights selected, called winning tickets, intact at the end of each training. However, WSN is inappropriate for sequential video compilation since it does not consider uncorrelated video contexts. To overcome the weakness of WSN, our PNR explores more appropriate weights for representing video with an additional random re-initialized step.

3 Progressive Neural Representation

This section presents our proposed continual neural implicit representation method, named *Progressive Neural Representation (PNR)*. Given a supernet backbone, where we follow a NeRV [21] architecture for video embedding and decoding, PNR aims to expand its representation space continuously by sequentially encoding multiple videos. As new videos arrive in the model, PNR jointly updates the binary masks with neural network weights searching for the adaptive subnetwork to encode given videos. After training each video session, we freeze the weights of the selected subnetwork so that future training does not hurt the quality of the learned representation and the generated output, even though the new subnetwork structure contains some weights already encoded in the previous video. While the weights learned in earlier video sessions are frozen, we enable our PNR to transfer prior knowledge to future video tasks (i.e., forward transfer). This makes the model adapt new videos effectively by leveraging the representation of past videos (Please see Figure 1).

Problem Statement. Let a video at s_{th} session $V_s = \{v_t^s\}_{t=1}^{T_s} \in \mathbb{R}^{T_s \times H \times W \times 3}$ be represented by a function with the trainable parameter θ , $f_\theta : \mathbb{R} \rightarrow \mathbb{R}^{H \times W \times 3}$, during Video Continual Learning (VCL), where T_s denotes the number of frames in a video at session s , and $s \in \{1 \dots, |S|\}$. Given a session and frame index s and t , respectively, the neural implicit representation aims to predict a corresponding RGB image $v_t^s \in \mathbb{R}^{H \times W \times 3}$ by fitting an encoding function to a neural network: $v_t^s = f_\theta([s; t])$. Let's consider a learning scenario that $|S| = N$ sessions arrive in the model sequentially. We denote that $\mathcal{D}_s = \{e_{s,t}, v_{s,t}\}_{t=1}^{T_s}$ is the dataset of session s , composed of T_s pairs of raw embeddings $e_{s,t} = [e_s; e_t]$ and corresponding frames v_t^s . Here, we assume that \mathcal{D}_s for session s is only accessible when learning session s due to the limited hardware memory and privacy-preserving issues, and session identity is given in the training and testing stages. The training objective of the suggested video continual learning on a sequence of N sessions is to minimize the following optimization problem:

$$\theta^* = \underset{\theta}{\text{minimize}} \frac{1}{N} \frac{1}{T_s} \sum_{s=1}^N \sum_{t=1}^{T_s} \mathcal{L}(f(e_{s,t}; \theta), v_t^s), \quad (1)$$

where the loss function $\mathcal{L}(v_t^s)$ is composed of ℓ_1 loss and *SSIM loss*. The former minimizes the pixel-wise RGB gap with the original input frames evenly, and the latter maximizes the similarity between the two entire frames based on luminance, contrast, and structure, as follows:

$$\mathcal{L}(V_s) = \frac{1}{T_s} \sum_{t=1}^{T_s} \alpha \|v_t^s - \hat{v}_t^s\|_1 + (1 - \alpha)(1 - \text{SSIM}(v_t^s, \hat{v}_t^s)), \quad (2)$$

where \hat{v}_t^s is the output generated by the model f . For all experiments, we set the hyperparameter α to 0.7, and we adapt PixelShuffle [37] for session and time positional embedding.

Continual learners frequently use over-parameterized deep neural networks to ensure enough capacity for learning future tasks. This approach often leads to the discovery of subnetworks that perform as well as or better than the original network. Given the neural network parameters θ , the binary attention mask \mathbf{m}_s^* that describes the optimal subnetwork for session t such that $|\mathbf{m}_s^*|$ is less than the model capacity c follows as:

$$\mathbf{m}_s^* = \underset{\mathbf{m}_s \in \{0,1\}^{|\theta|}}{\text{minimize}} \frac{1}{T_s} \sum_{t=1}^{T_s} \mathcal{L}(f(e_{s,t}; \theta \odot \mathbf{m}_s), v_t^s) - \mathcal{J}, \quad \text{subject to } |\mathbf{m}_s^*| \leq c, \quad (3)$$

where session loss $\mathcal{J} = \mathcal{L}(v_t^s)$ and $c \ll |\theta|$ (used as the selected proportion % of model parameters in the following section). In the optimization section, we describe how to obtain \mathbf{m}_s^* using a single learnable weight score ρ subject to updates while minimizing task loss jointly for each video session.

3.1 Sequential Video Representational Subnetworks

Let each weight be associated with a learnable parameter we call *weight score* ρ , which numerically determines the importance of the weight associated with it; that is, a weight with a higher weight score is seen as more important. We find a sparse subnetwork $\hat{\theta}_s$ of the neural network and assign it as a solver of the current session s . We use subnetworks instead of the dense network as solvers for two reasons: (1) Lottery Ticket Hypothesis [11] shows the existence of a competitive subnetwork

that is comparable with the dense network, and (2) the subnetwork requires less capacity than dense networks, and therefore it inherently reduces the size of the expansion of the solver.

Motivated by such benefits, we propose a novel PNR, the joint-training method for sequential video representation compilation, as shown in **Algorithm 1**. The pseudo-code explains how to acquire subnetworks within a dense network. We find $\hat{\theta}_s = \theta \odot \mathbf{m}_s$ by selecting the top- $c\%$ weights from the weight scores ρ , where c is the target layer-wise capacity ratio in %; \mathbf{m}_s is a session-dependent binary mask. Formally, \mathbf{m}_s is obtained by applying a indicator function $\mathbb{1}_c$ on ρ where $\mathbb{1}_c(\rho) = 1$ if ρ belongs to top- $c\%$ scores and 0 otherwise. Therefore, the subnetworks $\{\hat{\theta}_s\}_{s=1}^N$ for all video session \mathcal{S} are obtained by $\hat{\theta}_s = \theta \odot \mathbf{m}_s$. Straight-through estimator [1, 15, 30] is used to update ρ .

Algorithm 1 Progressive Neural Representation (PNR) for VCL

input: $\{\mathcal{D}_s\}_{s=1}^N$, model weights θ , score weights ρ , binary mask $\mathbf{M}_0 = \mathbf{0}^{|\theta|}$,
and layer-wise capacity $c\%$.

- 1: randomly initialize θ and ρ .
- 2: **for** session $s = 1, \dots, |\mathcal{S}|$ **do**
- 3: **if** $s > 1$ **then**
- 4: randomly re-initialize ρ .
- 5: **end if**
- 6: **for** batch $\mathbf{b}_t \sim \mathcal{D}_s$ **do**
- 7: obtain mask \mathbf{m}_s of the top- $c\%$ scores ρ at each layer
- 8: compute $\mathcal{L}(f(e_{s,t}; \theta \odot \mathbf{m}_s), \mathbf{b}_t)$, where input embedding, $e_{s,t} = [e_s; e_t]$.
- 9: $\theta \leftarrow \theta - \eta \left(\frac{\partial \mathcal{L}}{\partial \theta} \odot (\mathbf{1} - \mathbf{M}_{s-1}) \right)$ ▷ trainable weight update
- 10: $\rho \leftarrow \rho - \eta \left(\frac{\partial \mathcal{L}}{\partial \rho} \right)$ ▷ weight score update
- 11: **end for**
- 12: $\hat{\theta}_s = \theta \odot \mathbf{m}_s$
- 13: $\mathbf{M}_s \leftarrow \mathbf{M}_{s-1} \vee \mathbf{m}_s$ ▷ accumulate binary mask
- 14: **end for**

output: $\{\hat{\theta}_s\}_{s=1}^N$

4 Experiments

We validate our method on video benchmark datasets against continual learning baselines on Video Task-incremental Learning (VTL). We consider continual video representation learning with a multi-head configuration for all experiments in the paper. We follow the experimental setups in NeRV [8] and HNeRV [7].

Datasets. 1) *UVG of 8 Video Sessions*: We experiment on eight sequential videos to validate our PNR. The eight videos consist of one from the scikit-video and seven from the UVG dataset. The category index and order in UVG8 are as follows: 1.bunny, 2.beauty, 3.bosphorus, 4.bee, 5.jockey, 6.setgo, 7.shake, 8.yacht.

2) *UVG of 17 Video Sessions*: We conduct an extended experiment on 17 video sessions by adding 9 more videos to the UVG of 8 video sessions. The category index and order in UVG17 are as follows: 1.bunny, 2.city, 3.beauty, 4.focus, 5.bosphorus, 6.kids, 7.bee, 8.pan, 9.jockey, 10.lips, 11.setgo, 12.race, 13.shake, 14.river, 15.yacht, 16.sunbath, 17.twilight. Please refer to the supplementary material.

Architecture. We employ NeRV as our baseline architecture and follow its details for a fair comparison. After the positional encoding, we apply four sparse MLP layers on the output of the positional encoding layer, followed by five sparse NeRV blocks with upscale factors of 5, 2, 2, 2, 2. These sparse NeRV blocks decode 1280×720 frames from the 16×9 feature map obtained after the sparse MLP layers. For the upscaling method in the sparse NeRV blocks, we also adopt PixelShuffle [37]. The positional encoding for the video index s and frame index t is as follows:

$$\begin{aligned} \mathbf{\Gamma}(s, t) = [& \sin(b^0 \pi s), \cos(b^0 \pi s), \dots, \sin(b^{l-1} \pi s), \cos(b^{l-1} \pi s), \\ & \sin(b^0 \pi t), \cos(b^0 \pi t), \dots, \sin(b^{l-1} \pi t), \cos(b^{l-1} \pi t)], \end{aligned} \quad (4)$$

where the hyperparameters are set to $b = 1.25$ and $l = 80$ such that $\mathbf{\Gamma}(s, t) \in \mathbb{R}^{1 \times 160}$. As differences from the previous NeRV model, the first layer of the MLP has its input size expanded from 80 to 160 to incorporate both frame and video indices, and distinct head layers after the NeRV block are utilized

for each video. For the loss objective in Equation 2, α is set to 0.7. We evaluate the video quality, average video session quality, and backward transfer with two metrics: PSNR and MS-SSIM [43]. We implement our model in PyTorch and train it in full precision (FP32). All experiments are run with NVIDIA RTX8000. Please refer to the supplementary material for more experimental details.

Table 1: PSNR results of UVG8 (m-IDX) Video Sessions with average PSNR and Backward Transfer (BTW) of PSNR. Note that * denotes our reproduced results.

Method	Sessions								Avg. PSNR / BWT
	1	2	3	4	5	6	7	8	
STL, NeRV [7]	39.63	36.06	37.35	41.23	38.14	31.86	37.22	32.45	36.74 / -
STL, NeRV*	39.66	36.28	38.14	42.03	36.58	29.22	37.27	31.45	36.33 / -
EWC [19]*	10.19	11.15	14.47	8.39	12.21	10.27	9.97	23.98	12.58 / -17.59
iCaRL [31]*	30.84	26.30	27.28	34.48	20.90	17.28	30.33	24.64	26.51 / -3.90
PNR, c = 10.0 %, m-IDX=8	27.81	30.66	29.30	33.06	22.16	18.40	27.81	22.97	26.52 / 0.0
PNR, c = 30.0 %, m-IDX=8	31.37	32.19	29.92	33.62	22.82	18.96	28.43	23.40	27.59 / 0.0
PNR, c = 50.0 %, m-IDX=8	34.05	32.28	29.98	32.88	22.15	18.61	27.68	23.64	27.66 / 0.0
PNR, c = 70.0 %, m-IDX=8	35.62	32.08	29.46	31.37	21.60	18.13	27.33	22.61	27.28 / 0.0
PNR, c = 10.0 %, m-IDX=8, <i>reinit</i>	28.12	31.31	29.89	34.83	23.82	19.56	29.46	24.58	27.72 / 0.0
PNR, c = 30.0 %, m-IDX=8, <i>reinit</i>	31.36	32.91	31.42	36.39	24.93	20.58	30.78	25.25	29.20 / 0.0
PNR, c = 50.0 %, m-IDX=8, <i>reinit</i>	34.10	33.45	31.77	36.09	24.82	20.25	30.02	25.01	29.44 / 0.0
PNR, c = 70.0 %, m-IDX=8, <i>reinit</i>	35.55	33.04	30.44	32.11	23.00	19.02	28.09	23.52	28.10 / 0.0
PNR, c = 10.0 %, m-IDX=17	27.68	30.29	28.66	31.62	21.05	17.85	27.07	22.98	25.90 / 0.0
PNR, c = 30.0 %, m-IDX=17	31.50	31.00	29.26	31.96	22.07	18.34	27.21	23.09	26.80 / 0.0
PNR, c = 50.0 %, m-IDX=17	34.02	31.04	28.95	31.26	21.93	18.22	26.88	22.72	26.87 / 0.0
PNR, c = 70.0 %, m-IDX=17	35.64	30.26	27.99	29.88	20.79	17.63	26.68	22.34	26.40 / 0.0
MLT	34.22	32.79	32.34	38.33	25.30	22.44	33.73	27.05	30.78 / -

Table 2: MS-SSIM results of UVG8 (m-IDX) Video Sessions with average MS-SSIM, Backward Transfer (BTW) of MS-SSIM. Note that * denotes our reproduced results.

Method	Sessions								Avg. MS-SSIM / BWT
	1	2	3	4	5	6	7	8	
STL, NeRV*	0.99	0.95	0.98	0.99	0.97	0.96	0.98	0.96	0.97/-
EWC [19]*	0.22	0.23	0.35	0.10	0.27	0.19	0.21	0.79	0.30 / -0.62
iCaRL [31]*	0.94	0.80	0.82	0.97	0.59	0.57	0.92	0.81	0.80 / -0.11
PNR, c = 10.0 %, m-IDX=8	0.91	0.89	0.89	0.97	0.73	0.61	0.88	0.77	0.83 / 0.0
PNR, c = 30.0 %, m-IDX=8	0.96	0.91	0.90	0.98	0.76	0.65	0.89	0.78	0.85 / 0.0
PNR, c = 50.0 %, m-IDX=8	0.98	0.91	0.90	0.97	0.74	0.62	0.88	0.77	0.85 / 0.0
PNR, c = 70.0 %, m-IDX=8	0.98	0.91	0.89	0.96	0.71	0.59	0.87	0.74	0.83 / 0.0
PNR, c = 10.0 %, m-IDX=8, <i>reinit</i>	0.91	0.90	0.90	0.98	0.78	0.68	0.91	0.81	0.86 / 0.0
PNR, c = 30.0 %, m-IDX=8, <i>reinit</i>	0.96	0.99	0.92	0.99	0.82	0.74	0.93	0.84	0.89 / 0.0
PNR, c = 50.0 %, m-IDX=8, <i>reinit</i>	0.98	0.92	0.93	0.98	0.82	0.72	0.92	0.83	0.89 / 0.0
PNR, c = 70.0 %, m-IDX=8, <i>reinit</i>	0.98	0.92	0.91	0.97	0.76	0.65	0.89	0.79	0.86 / 0.0
PNR, c = 10.0 %, m-IDX=17	0.90	0.88	0.87	0.96	0.69	0.57	0.86	0.74	0.80 / 0.0
PNR, c = 30.0 %, m-IDX=17	0.96	0.89	0.88	0.97	0.73	0.60	0.86	0.76	0.83 / 0.0
PNR, c = 50.0 %, m-IDX=17	0.98	0.89	0.88	0.96	0.73	0.60	0.85	0.75	0.83 / 0.0
PNR, c = 70.0 %, m-IDX=17	0.98	0.88	0.85	0.95	0.68	0.55	0.85	0.73	0.81 / 0.0
MLT	0.98	0.91	0.93	0.99	0.84	0.82	0.95	0.89	0.91 / -

Baselines. To show the effectiveness, we compare our PNR with strong CL baselines; Single-Task Learning (STL) which trains on single tasks independently, EWC [19], which is a regularized baseline, iCaRL [31] which is a rehearsal-based baseline, and Multi-Task Learning (MTL) which trains on multiple video sessions simultaneously, showing the upper-bound of PNR. Except for STL, all models are trained and evaluated on multi-head settings where a video session and time (s, t) indices are provided.

Training. In all experiments, we follow the same experimental settings as NeRV [7] and HNeRV [7] for fair comparisons. We train the PNR, NeRV (STL), and MTL using Adam optimizer with a learning rate $5e-4$. For the ablation study on UVG8 and UVG17, we use a cosine annealing learning rate schedule [22], batch size of 1, training epochs of 150, and warmup epochs of 30 unless otherwise denoted.

Performance metrics of PSNR & MS-SSIM. We evaluate all methods based on the following continual learning metrics:

1. *Average PSNR or MS-SSIM (i.e., Ave. PSNR)* measures the average of the final performances on all video sessions: $PSNR \text{ or } MS-SSIM = \frac{1}{N} \sum_{s=1}^N R_{S,s}$, where $R_{S,s}$ is the test PSNR or MS-SSIM for session s after training on the final video session S .

2. *Backward Transfer of PSNR or MS-SSIM (BWT)* measures the video representation forgetting during continual learning. Negative BWT means that learning new video sessions causes the video representation forgetting of past sessions: $BWT = \frac{1}{S-1} \sum_{s=1}^{S-1} R_{S,s} - R_{s,s}$.

Table 3: PSNR results of UVG17 (m-IDX) Video Sessions with average PSNR and Backward Transfer (BTW) of PSNR. Note that * denotes our reproduced results.

Method	Sessions																	Avg. MS-SSIM BWT
	1	2	3	4	5	6	7	8	9	10	11	12	13	14	15	16	17	
STL, NeRV [7]	39.63	-	36.06	-	37.35	-	41.23	-	38.14	-	31.86	-	37.22	-	32.45	-	-	- / -
STL, NeRV*	39.66	44.89	36.28	41.13	38.14	31.53	42.03	34.74	36.58	36.85	29.22	31.81	37.27	34.18	31.45	38.41	43.86	36.94 / -
EWC [19]*	11.15	9.21	12.71	11.40	15.58	9.25	7.06	12.96	6.34	10.31	9.55	13.39	5.76	8.67	10.93	10.92	28.29	11.38 / -16.13
iCaRL [31]*	24.31	28.25	22.19	22.74	22.84	16.55	29.37	17.92	16.65	27.43	13.64	16.42	24.02	21.60	19.40	18.60	26.46	21.67 / -6.23
PNR, c = 10.0 %	27.68	31.31	30.29	31.63	28.66	22.57	31.62	22.04	21.05	32.71	17.85	20.09	27.07	23.84	22.98	20.50	28.56	25.91 / 0.0
PNR, c = 30.0 %	31.50	34.37	31.00	32.38	29.26	23.08	31.96	22.64	22.07	33.48	18.34	20.45	27.21	24.33	23.09	21.23	29.13	26.80 / 0.0
PNR, c = 50.0 %	34.02	34.93	31.04	31.74	28.95	23.07	31.26	22.32	21.93	33.35	18.22	20.34	26.88	24.22	22.72	21.30	28.86	26.77 / 0.0
PNR, c = 70.0 %	35.64	34.36	30.26	30.27	27.99	22.55	29.88	21.46	20.79	32.37	17.63	20.00	26.68	23.79	22.34	20.69	28.68	26.20 / 0.0
PNR, c = 10.0 %, <i>reinit</i>	28.02	32.68	31.38	33.13	29.54	23.75	33.91	24.49	23.63	34.91	19.42	21.71	29.09	26.14	24.47	23.57	31.34	27.72 / 0.0
PNR, c = 30.0 %, <i>reinit</i>	31.47	35.42	32.51	34.73	30.70	24.53	35.63	25.49	24.50	35.59	20.24	22.49	30.22	27.03	25.14	24.86	32.16	28.98 / 0.0
PNR, c = 50.0 %, <i>reinit</i>	34.05	36.61	32.73	34.99	30.43	24.37	33.98	24.53	24.31	35.51	19.99	22.31	29.65	26.77	24.94	24.76	31.84	28.93 / 0.0
PNR, c = 70.0 %, <i>reinit</i>	35.57	35.93	31.61	31.39	28.32	23.19	30.40	22.69	22.70	34.69	18.82	21.09	27.75	25.43	23.47	23.24	30.30	27.45 / 0.0
MLT	32.39	34.35	31.45	34.03	30.70	24.53	37.13	27.83	23.80	34.69	20.77	22.37	32.71	28.00	25.89	26.40	33.16	29.42 / -

Table 4: MS-SSIM results of UVG17 (m-IDX) Video Sessions with average MS-SSIM and Backward Transfer (BTW) of MS-SSIM. Note that * denotes our reproduced results.

Method	Sessions																	Avg. MS-SSIM BWT
	1	2	3	4	5	6	7	8	9	10	11	12	13	14	15	16	17	
STL, NeRV*	0.99	0.99	0.95	0.98	0.98	0.96	0.99	0.98	0.97	0.95	0.96	0.96	0.98	0.98	0.96	0.99	0.99	0.97 / -
EWC [19]*	0.26	0.24	0.44	0.24	0.40	0.29	0.15	0.17	0.26	0.26	0.17	0.34	0.04	0.30	0.33	0.31	0.91	0.30 / -0.55
iCaRL [31]*	0.74	0.88	0.67	0.67	0.64	0.48	0.91	0.53	0.37	0.82	0.35	0.53	0.75	0.70	0.61	0.60	0.87	0.65 / -0.20
PNR, c = 10.0 %	0.90	0.94	0.88	0.92	0.87	0.75	0.96	0.74	0.69	0.91	0.57	0.72	0.86	0.80	0.74	0.69	0.92	0.82 / 0.0
PNR, c = 30.0 %	0.96	0.97	0.89	0.93	0.88	0.77	0.97	0.77	0.73	0.91	0.60	0.74	0.86	0.81	0.76	0.72	0.93	0.84 / 0.0
PNR, c = 50.0 %	0.98	0.97	0.89	0.92	0.88	0.77	0.96	0.75	0.73	0.91	0.60	0.74	0.85	0.80	0.75	0.73	0.92	0.83 / 0.0
PNR, c = 70.0 %	0.98	0.97	0.88	0.91	0.85	0.75	0.95	0.70	0.68	0.91	0.55	0.72	0.85	0.80	0.73	0.70	0.92	0.82 / 0.0
PNR, c = 10.0 %, <i>reinit</i>	0.91	0.96	0.90	0.94	0.89	0.80	0.98	0.84	0.78	0.93	0.68	0.78	0.91	0.86	0.81	0.82	0.96	0.87 / 0.0
PNR, c = 30.0 %, <i>reinit</i>	0.96	0.98	0.91	0.95	0.91	0.83	0.98	0.87	0.81	0.93	0.72	0.81	0.92	0.88	0.83	0.86	0.97	0.89 / 0.0
PNR, c = 50.0 %, <i>reinit</i>	0.98	0.98	0.91	0.91	0.95	0.91	0.82	0.98	0.85	0.80	0.93	0.71	0.80	0.91	0.88	0.83	0.86	0.89 / 0.0
PNR, c = 70.0 %, <i>reinit</i>	0.98	0.98	0.90	0.92	0.87	0.78	0.95	0.77	0.76	0.92	0.64	0.77	0.88	0.84	0.79	0.81	0.95	0.85 / 0.0
MLT	0.97	0.97	0.90	0.94	0.91	0.82	0.99	0.92	0.80	0.92	0.75	0.81	0.94	0.90	0.85	0.89	0.97	0.90 / -

4.1 Comparisons with Baselines

PSNR & MS-SSIM. To compare PNR with conventional representative continual learning methods such as EWC and iCaRL, we prepare the reproduced results, as shown in Tables 1, 2, 3, and 4. The PNR outperforms the conventional baselines on the UVG8 and UVG17 benchmark datasets. The sparseness does not significantly affect sequential video representation results on two sequential benchmark datasets. Moreover, our performances of PNR with reinit are better than those of PNR without reinit, comparable with those of MLT (upper-bound of PNR).

Input Embedding. We observe that the input embedding resolutions affect video representation as shown in Table 1 and Table 2. Even though the video sessions are the same, the performances of PSNR and MS-SSIM decrease by 0.8, 0.2, depending on input embedding resolution determined by the maximum number of input index (m-IDX). The results with m-IDX=17 are reported by the longer sequence learning in Table 3 and Table 4. From this observation, we can expect more precise video representation if we use more discriminative input embedding for PNR. Here, we do not care about the video’s contextual information.

Transfer Matrix. We prepare the transfer matrix to prove our PNR’s forget-freeness and to show video correlation among other videos, as shown in Figure 2 on the UVG17 dataset; lower triangular estimated by each session subnetwork denotes that our PNR is a forget-free method and upper triangular calculated by current session subnetwork denotes the video similarity between source and target. The reinitialized PNR proves the effectiveness from the lower triangular of Figure 2 (a) and (b). Nothing special is observable from the upper triangular since they are not correlated.

PNR’s Compression. We follow NeRV’s video quantization and compression pipeline [8], except for the model pruning step, to evaluate performance drops and backward transfer in the video sequential learning, as shown in Figure 3. Once sequential training is done, our PNR doesn’t need any extra

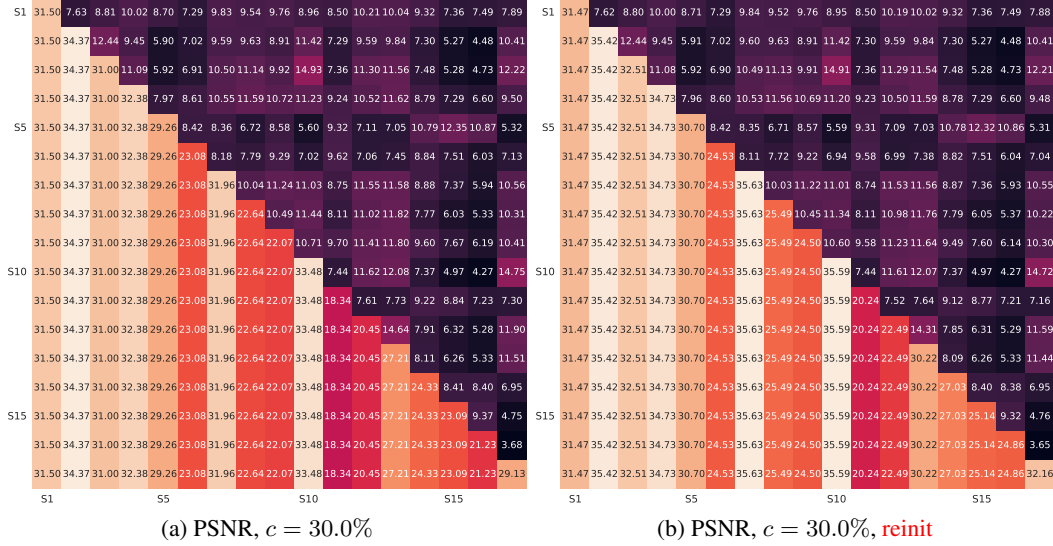


Figure 2: PNR’s Transfer Matrixes of PSNR on the UVG17 dataset.

prune and finetune steps, unlike NeRV. This point is our key advantage of PNR over NeRV. Figure 3 (a) shows the results of various sparsity and bit-quantization on the UVG17 datasets: the 8bit of PNR’s performances are comparable with 32bit of ones without a significant video quality drop. Figure 3 (b) shows the rate-distortion curves. We compare PNR (reinit) with PNR and NeRV (STL). For a fair comparison, we take steps of pruning, fine-tuning, quantizing, and encoding NeRV. Our PNR (reinit) outperforms all baselines.

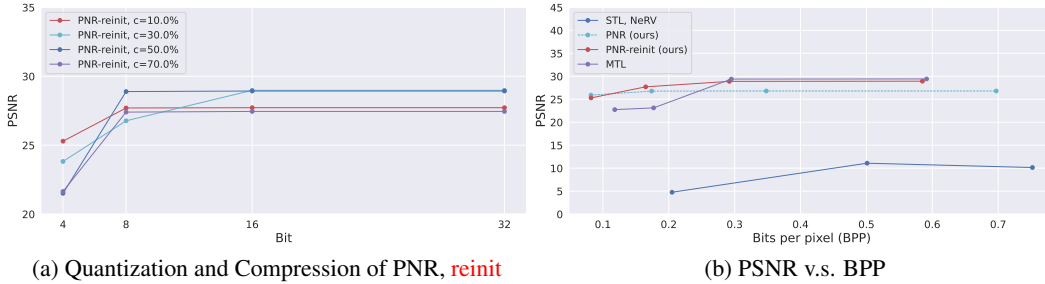


Figure 3: PSNR v.s. Bits-per-pixel (BPP) on the UVG17 datasets

PNR’s Capacity. We prepare a video session-wise PSNR and investigate how PNR reuses weights over sequential video sessions, as shown in Figure 4 (b). PNR tends to progressively transfer weights used for a prior session to weights for new ones compared with others, i.e., PNR with reinit. Since the reinitialized PNR explores more new weights than PNR, PNR with reinit outperforms PNR, as stated in Figure 4 (a), leading to comparable with MTL. This result might suggest that properly reused weights lead to generalization more than others in VCL with low video contextual similarity.

4.2 PNR’s Video Generation

We prepare the results of video generation as shown in Figure 5. We demonstrate that a sparse solution (PNR with $c = 30.0\%$, reinit) generates video representations sequentially without significant performance drops, compared with MLT’s results. Please refer to the supplementary material for more visualizations and comparisons with baselines.

5 Conclusion

Neural Implicit Representations (NIR) have gained significant attention recently due to their ability to represent complex and high-dimensional data. Unlike explicit representations, which require storing

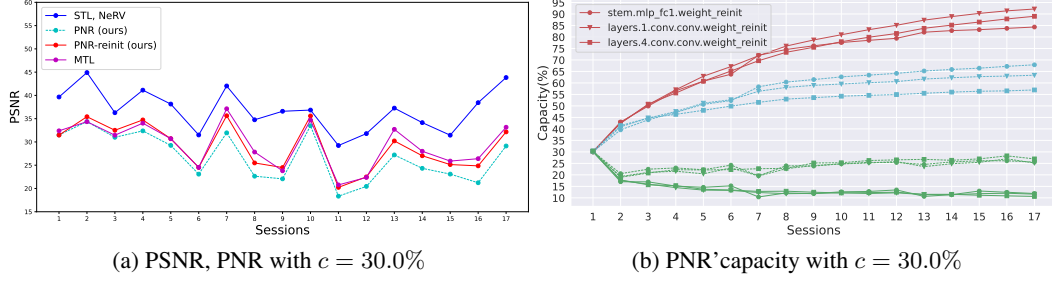


Figure 4: PNR’s Comparison of PSNR with others and layer-wise accumulated Capacities on the UVG17 dataset. Note that **green** represents a reused subnetwork at the current session (s) obtained at the past (s-1) video sessions in (b): **reinit** (solid line) v.s **non-reinit** (dashed line).

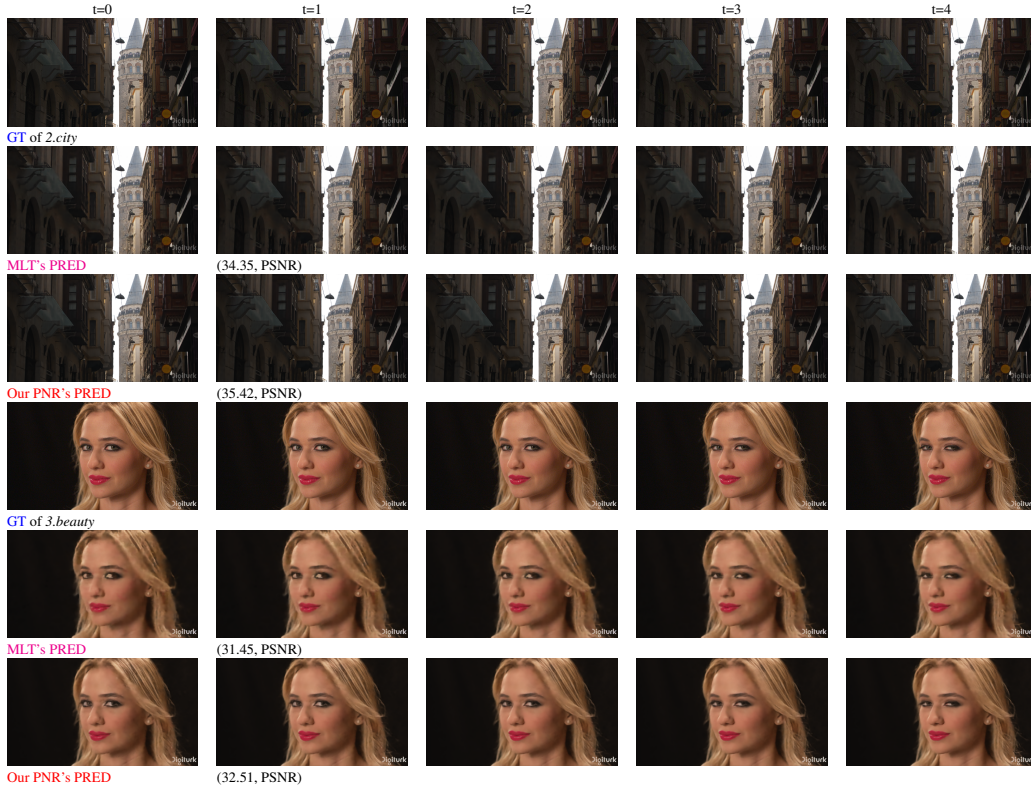


Figure 5: PNR’s Video Generation (from t=0 to t=2) with $c = 30.0\%$ and **reinit** on the UVG17 dataset. Note that **GT**: ground-truth and **PRED**: model’s predictions. The PSNR denotes each video session’s scores in Table 3.

and manipulating individual data points, implicit representations capture information through a learned mapping function without explicitly representing the data points themselves. While they often compress neural networks substantially to accelerate encoding/decoding speed, yet existing methods fail to transfer learned representations to new videos. This work investigates the continuous expansion of implicit video representations as videos arrive sequentially over time, where the model can only access the videos from the current session. To tackle this problem, we propose a novel neural video representation, *Progressive Neural Representation (PNR)*, that finds an adaptive substructure from the supernet to the given video based on Lottery Ticket Hypothesis. At each training session, our PNR transfers the learned knowledge of the previously obtained subnetworks to obtain the representation of the current video without modifying past subnetwork weights. Therefore it can perfectly preserve the decoding ability (i.e., catastrophic forgetting) on previous videos. We demonstrate the effectiveness of our proposed PNR over baselines on the novel UVG8/17 video sequence benchmark datasets.

References

- [1] Yoshua Bengio, Nicholas Léonard, and Aaron C. Courville. Estimating or propagating gradients through stochastic neurons for conditional computation. *CoRR*, 2013. 5
- [2] Arslan Chaudhry, Naeemullah Khan, Puneet K Dokania, and Philip HS Torr. Continual learning in low-rank orthogonal subspaces. In *Advances in Neural Information Processing Systems (NeurIPS)*, 2020. 2
- [3] Arslan Chaudhry, Marc’Aurelio Ranzato, Marcus Rohrbach, and Mohamed Elhoseiny. Efficient lifelong learning with a-gem. In *Proceedings of the International Conference on Learning Representations (ICLR)*, 2019. 3
- [4] Arslan Chaudhry, Marcus Rohrbach, Mohamed Elhoseiny, Thalaiyasingam Ajanthan, Puneet K Dokania, Philip HS Torr, and M Ranzato. Continual learning with tiny episodic memories. *arXiv preprint arXiv:1902.10486*, 2019. 2
- [5] Geng Chen, Wendong Zhang, Han Lu, Siyu Gao, Yunbo Wang, Mingsheng Long, and Xiaokang Yang. Continual predictive learning from videos. In *Proceedings of the IEEE/CVF Conference on Computer Vision and Pattern Recognition*, pages 10728–10737, 2022. 3
- [6] Hao Chen, Matt Gwilliam, Bo He, Ser-Nam Lim, and Abhinav Shrivastava. Cnerv: Content-adaptive neural representation for visual data. *arXiv preprint arXiv:2211.10421*, 2022. 1, 3
- [7] Hao Chen, Matt Gwilliam, Ser-Nam Lim, and Abhinav Shrivastava. Hnerv: A hybrid neural representation for videos. *arXiv preprint arXiv:2304.02633*, 2023. 1, 3, 5, 6, 7
- [8] Hao Chen, Bo He, Hanyu Wang, Yixuan Ren, Ser Nam Lim, and Abhinav Shrivastava. Nerv: Neural representations for videos. *Advances in Neural Information Processing Systems*, 34:21557–21568, 2021. 1, 3, 5, 7
- [9] Tianlong Chen, Zhenyu Zhang, Sijia Liu, Shiyu Chang, and Zhangyang Wang. Long live the lottery: The existence of winning tickets in lifelong learning. In *Proceedings of the International Conference on Learning Representations (ICLR)*, 2021. 3
- [10] Zhiqin Chen and Hao Zhang. Learning implicit fields for generative shape modeling. In *Proceedings of the IEEE/CVF Conference on Computer Vision and Pattern Recognition*, pages 5939–5948, 2019. 2
- [11] Jonathan Frankle and Michael Carbin. The lottery ticket hypothesis: Finding sparse, trainable neural networks. In *Proceedings of the International Conference on Learning Representations (ICLR)*, 2019. 4
- [12] Siavash Golkar, Michael Kagan, and Kyunghyun Cho. Continual learning via neural pruning. *arXiv preprint arXiv:1903.04476*, 2019. 3
- [13] Demis Hassabis, Dharmashan Kumaran, Christopher Summerfield, and Matthew Botvinick. Neuroscience-inspired artificial intelligence. *Neuron*, 95(2):245–258, 2017. 2
- [14] Bo He, Xitong Yang, Hanyu Wang, Zuxuan Wu, Hao Chen, Shuaiyi Huang, Yixuan Ren, Ser-Nam Lim, and Abhinav Shrivastava. Towards scalable neural representation for diverse videos. *arXiv preprint arXiv:2303.14124*, 2023. 3
- [15] Geoffrey Hinton. Neural networks for machine learning, 2012. 5
- [16] Sangwon Jung, Hongjoon Ahn, Sungmin Cha, and Taesup Moon. Continual learning with node-importance based adaptive group sparse regularization. In *Advances in Neural Information Processing Systems (NeurIPS)*, 2020. 2
- [17] Haeyong Kang, Rusty John Lloyd Mina, Sultan Rizky Hikmawan Madjid, Jaehong Yoon, Mark Hasegawa-Johnson, Sung Ju Hwang, and Chang D Yoo. Forget-free continual learning with winning subnetworks. In *International Conference on Machine Learning*, pages 10734–10750. PMLR, 2022. 2, 3
- [18] Haeyong Kang, Jaehong Yoon, Sultan Rizky Hikmawan Madjid, Sung Ju Hwang, and Chang D Yoo. On the soft-subnetwork for few-shot class incremental learning. *arXiv preprint arXiv:2209.07529*, 2022. 2

- [19] James Kirkpatrick, Razvan Pascanu, Neil Rabinowitz, Joel Veness, Guillaume Desjardins, Andrei A Rusu, Kieran Milan, John Quan, Tiago Ramalho, Agnieszka Grabska-Barwinska, Demis Hassabis, Claudia Clopath, Dharshan Kumaran, and Raia Hadsell. Overcoming catastrophic forgetting in neural networks. 2017. 2, 6, 7
- [20] Xilai Li, Yingbo Zhou, Tianfu Wu, Richard Socher, and Caiming Xiong. Learn to grow: A continual structure learning framework for overcoming catastrophic forgetting. In *Proceedings of the International Conference on Machine Learning (ICML)*, 2019. 3
- [21] Zizhang Li, Mengmeng Wang, Huaijin Pi, Kechun Xu, Jianbiao Mei, and Yong Liu. E-nerv: Expedite neural video representation with disentangled spatial-temporal context. In *Computer Vision–ECCV 2022: 17th European Conference, Tel Aviv, Israel, October 23–27, 2022, Proceedings, Part XXXV*, pages 267–284. Springer, 2022. 1, 3, 4
- [22] Ilya Loshchilov and Frank Hutter. Sgdr: Stochastic gradient descent with warm restarts. *arXiv preprint arXiv:1608.03983*, 2016. 6
- [23] Shishira R Maiya, Sharath Girish, Max Ehrlich, Hanyu Wang, Kwot Sin Lee, Patrick Poirson, Pengxiang Wu, Chen Wang, and Abhinav Shrivastava. Nirvana: Neural implicit representations of videos with adaptive networks and autoregressive patch-wise modeling. *arXiv preprint arXiv:2212.14593*, 2022. 3
- [24] Arun Mallya, Dillon Davis, and Svetlana Lazebnik. Piggyback: Adapting a single network to multiple tasks by learning to mask weights. In *Proceedings of the European Conference on Computer Vision (ECCV)*, 2018. 2, 3
- [25] Michael McCloskey and Neal J Cohen. Catastrophic interference in connectionist networks: The sequential learning problem. In *Psychology of learning and motivation*, volume 24, pages 109–165. Elsevier, 1989. 2
- [26] Ishit Mehta, Michaël Gharbi, Connelly Barnes, Eli Shechtman, Ravi Ramamoorthi, and Manmohan Chandraker. Modulated periodic activations for generalizable local functional representations. In *Proceedings of the IEEE/CVF International Conference on Computer Vision*, pages 14214–14223, 2021. 1, 2
- [27] Ben Mildenhall, Pratul P Srinivasan, Matthew Tancik, Jonathan T Barron, Ravi Ramamoorthi, and Ren Ng. Nerf: Representing scenes as neural radiance fields for view synthesis. *Communications of the ACM*, 65(1):99–106, 2021. 2
- [28] Seyed Iman Mirzadeh, Mehrdad Farajtabar, Dilan Gorur, Razvan Pascanu, and Hassan Ghasemzadeh. Linear mode connectivity in multitask and continual learning. In *Proceedings of the International Conference on Learning Representations (ICLR)*, 2021. 2
- [29] Jeong Joon Park, Peter Florence, Julian Straub, Richard Newcombe, and Steven Lovegrove. DeepSDF: Learning continuous signed distance functions for shape representation. In *Proceedings of the IEEE/CVF conference on computer vision and pattern recognition*, pages 165–174, 2019. 2
- [30] Vivek Ramanujan, Mitchell Wortsman, Aniruddha Kembhavi, Ali Farhadi, and Mohammad Rastegari. What’s hidden in a randomly weighted neural network? In *Proceedings of the IEEE International Conference on Computer Vision and Pattern Recognition (CVPR)*, 2020. 5
- [31] Sylvestre-Alvise Rebuffi, Alexander Kolesnikov, Georg Sperl, and Christoph H Lampert. icarl: Incremental classifier and representation learning. In *Proceedings of the IEEE conference on Computer Vision and Pattern Recognition*, pages 2001–2010, 2017. 2, 6, 7
- [32] Matthew Riemer, Ignacio Cases, Robert Ajemian, Miao Liu, Irina Rish, Yuhai Tu, and Gerald Tesauero. Learning to learn without forgetting by maximizing transfer and minimizing interference. *arXiv preprint arXiv:1810.11910*, 2018. 3
- [33] Andrei A Rusu, Neil C Rabinowitz, Guillaume Desjardins, Hubert Soyer, James Kirkpatrick, Koray Kavukcuoglu, Razvan Pascanu, and Raia Hadsell. Progressive neural networks. *arXiv preprint arXiv:1606.04671*, 2016. 2
- [34] Gobinda Saha, Isha Garg, and Kaushik Roy. Gradient projection memory for continual learning. In *Proceedings of the International Conference on Learning Representations (ICLR)*, 2021. 2
- [35] Katja Schwarz, Yiyi Liao, Michael Niemeyer, and Andreas Geiger. Graf: Generative radiance fields for 3d-aware image synthesis. *Advances in Neural Information Processing Systems*, 33:20154–20166, 2020. 2

- [36] Joan Serra, Didac Suris, Marius Miron, and Alexandros Karatzoglou. Overcoming catastrophic forgetting with hard attention to the task. In *Proceedings of the International Conference on Machine Learning (ICML)*, 2018. 2, 3
- [37] Wenzhe Shi, Jose Caballero, Ferenc Huszár, Johannes Totz, Andrew P Aitken, Rob Bishop, Daniel Rueckert, and Zehan Wang. Real-time single image and video super-resolution using an efficient sub-pixel convolutional neural network. In *Proceedings of the IEEE conference on computer vision and pattern recognition*, pages 1874–1883, 2016. 4, 5
- [38] Vincent Sitzmann, Julien Martel, Alexander Bergman, David Lindell, and Gordon Wetzstein. Implicit neural representations with periodic activation functions. *Advances in Neural Information Processing Systems*, 33:7462–7473, 2020. 2
- [39] Matthew Tancik, Pratul Srinivasan, Ben Mildenhall, Sara Fridovich-Keil, Nithin Raghavan, Utkarsh Singhal, Ravi Ramamoorthi, Jonathan Barron, and Ren Ng. Fourier features let networks learn high frequency functions in low dimensional domains. *Advances in Neural Information Processing Systems*, 33:7537–7547, 2020. 2
- [40] Sebastian Thrun. *A Lifelong Learning Perspective for Mobile Robot Control*. Elsevier, 1995. 2
- [41] Michalis K Titsias, Jonathan Schwarz, Alexander G de G Matthews, Razvan Pascanu, and Yee Whye Teh. Functional regularisation for continual learning with gaussian processes. In *Proceedings of the International Conference on Learning Representations (ICLR)*, 2020. 2
- [42] Andrés Villa, Juan León Alcázar, Motasem Alfarra, Kumail Alhamoud, Julio Hurtado, Fabian Caba Heilbron, Alvaro Soto, and Bernard Ghanem. Pivot: Prompting for video continual learning. *arXiv preprint arXiv:2212.04842*, 2022. 3
- [43] Zhou Wang, Eero P Simoncelli, and Alan C Bovik. Multiscale structural similarity for image quality assessment. In *The Thirty-Seventh Asilomar Conference on Signals, Systems & Computers*, 2003, volume 2, pages 1398–1402. Ieee, 2003. 6
- [44] Mitchell Wortsman, Vivek Ramanujan, Rosanne Liu, Aniruddha Kembhavi, Mohammad Rastegari, Jason Yosinski, and Ali Farhadi. Supermasks in superposition. In *Advances in Neural Information Processing Systems (NeurIPS)*, 2020. 2
- [45] Jaehong Yoon, Saehoon Kim, Eunho Yang, and Sung Ju Hwang. Scalable and order-robust continual learning with additive parameter decomposition. In *Proceedings of the International Conference on Learning Representations (ICLR)*, 2020. 3
- [46] Jaehong Yoon, Divyam Madaan, Eunho Yang, and Sung Ju Hwang. Online coreset selection for rehearsal-based continual learning. In *Proceedings of the International Conference on Learning Representations (ICLR)*, 2022. 2
- [47] Jaehong Yoon, Eunho Yang, Jeongtae Lee, and Sung Ju Hwang. Lifelong learning with dynamically expandable networks. In *Proceedings of the International Conference on Learning Representations (ICLR)*, 2018. 2
- [48] Friedemann Zenke, Ben Poole, and Surya Ganguli. Continual learning through synaptic intelligence. In *International Conference on Machine Learning*, pages 3987–3995. PMLR, 2017. 2